

Dietary material properties shape cranial suture morphology in the mouse calvarium

Craig Byron,[†]  Meghan Segreti, Katelyn Hawkinson, Katelyn Herman and Shivam Patel

Department of Biology, Mercer University, Macon, GA, USA

Abstract

Cranial sutures are fibrous connective tissue articulations found between intramembranous bones of the vertebrate cranium. Growth and remodeling of these tissues is partially regulated by biomechanical loading patterns that include stresses related to chewing. Advances in oral processing structure and function of the cranium that enabled mammalian-style chewing is commonly tied to the origins and evolution of this group. To what degree masticatory overuse or underuse shapes the complexity and ossification around these articulations can be predicted based on prior experimental and comparative work. Here, we report on a mouse model system that has been used to experimentally manipulate dietary material properties in order to investigate cranial suture morphology. Experimental groups were fed diets of contrasting material properties. A masticatory overuse group was fed pelleted rodent chow, nuts with shells, and given access to cotton bedding squares. An underuse group was deprived of cotton bedding as well as diverse textured food, and instead received gelatinized food continuously. Animals were raised from weaning to adulthood on these diets, and sagittal, coronal and lambdoid suture morphology was compared between groups. Predicted intergroup variation was observed in mandibular corpus size and calvarial suture morphology, suggesting that masticatory overuse is associated with jaw and suture growth. The anterior region of the sagittal suture where it intersects with the coronal suture (bregma) showed no effect from the experiment. The posterior sagittal suture where it intersects with the lambdoid sutures (lambda) was more complex in the overuse group. In other words, the posterior calvarium was responsive to dietary material property demands while the anterior calvarium was not. This probably resulted from the different strain magnitudes and/or strain frequencies that occurred during overuse diets with diverse material properties as compared with underuse diets deprived of such enrichment. This work highlights the contrasting pattern of the sutural response to loading differences within the calvarium as a result of diet.

Key words: complexity; cranial sutures; diet; lambdoid; mouse; sagittal.

Introduction

Cranial sutures are fibrous connective tissue articulations found between intramembranous bones of the vertebrate cranium. Throughout development they serve as important cranial growth sites. The factors that regulate this growth are both genetic and environmental, as outlined by Moss (1997a,b,c,d). Of the environmental influences thought to play a role in suture growth, the mechanical factors that

result from feeding are likely to be important. The unique shape of sutures, whereby convex and concave bony lingu-lae along the border of one cranial bone interdigitate with the corresponding convexities and concavities of another, suggests some kind of morphogenetic coordination across the suture (Zollikofer & Weissmann, 2011; Khonsari et al. 2013) responsible for bone deposition and bone resorption there (Byron et al. 2004; Byron, 2006).

These cranial joints exhibit either straight or irregular bony margins that can be measured in three dimensions (x , y and z). A cross-section in the x - and z -axes from endocranial to ectocranial surfaces demonstrate sutures that are straight, overlapped or interdigitated (Markey et al. 2006). In studies using model systems, the cross-sectional (x - z) interdigitation of the suture appears to correlate to specific mechanical deformation patterns (Herring, 1972; Herring & Mucci, 1991; Rafferty & Herring, 1999; Sun et al. 2004). Herring and colleagues used a miniature swine model to

Correspondence

Craig D. Byron, Department of Biology, Mercer University, 1501 Mercer University Dr., Macon, GA 31207, USA. T: 478.301.2163; F: 478.301.2067; E: byron_cd@mercer.edu

[†]All animal usage was approved by Mercer's Institutional Care and Use Committee (IACUC#A1308012).

Accepted for publication 22 August 2018
Article published online 9 October 2018

associate compressive strains with sutures that interdigitate from endocranial to ectocranial surfaces. In contrast, tensile strains were associated with suture cross-sections observed to be straight or overlapping. Additionally, collagen fibers of the suture ligament arrange into fan-shape insertions with an orientation to best resist these strain energies (Rafferty & Herring, 1999; Jasinowski et al. 2010; Khonsari et al. 2013). The relationship of suture cross-sectional interdigitation with compression, and straight-edged abutment with tension, has also been observed in polypteriform fish (Markey et al. 2006; Markey & Marshall, 2007a,b). However, in *Polypterus* peak sutural strains were recorded at maximum gape and during suction feeding and not during biting (Markey et al. 2006). For amniote vertebrates that feed in terrestrial settings such as mammals, feeding does not involve suction; instead oral processing is typical of food items and peak strains are recorded during the slow close phase of the gape cycle (Weijs & de Jongh, 1977; Hylander et al. 1987). Nevertheless, during both biting and suction feeding in fish, tension defined the strain regime within the interfrontal suture which was straight in cross-section, while compression predominated in the interparietal suture which exhibits cross-sectional interdigitation (Markey et al. 2006; Markey & Marshall, 2007a,b).

Ligamentous connective tissues sutures have a composition of collagen fibers positioned between two opposing bone surfaces. Each fibrous structure is a dynamic area where cell and tissue activity interact with physical forces transmitted through adjacent and rigid bone mineral (Mao, 2002; Zollikofer & Weissmann, 2011). In fact, regions where sutures intersect likely focus, or concentrate, mechanical forces from multiple directions. It is in this zone where a mechanical load meets more compliant tissue allowing for deformation along multiple orthogonal axes (Curtis et al. 2013; Cuff et al. 2015). To what degree masticatory overuse or underuse shapes the complexity and ossification around these articulations can be predicted based on prior work. Across a diverse array of vertebrates, cranial suture complexity tends to be greater in taxa specialized for enhanced craniofacial use, including eating hard and obdurate foods (Monteiro & Lessa, 2000; Byron, 2009), antler-sparring/head-butting (Jaslow, 1990; Jaslow & Biewener, 1995; Farke, 2008), fossorial lifestyles (Buezas et al. 2017), and even animals with experimentally strengthened masticatory muscles (Byron et al. 2004; Byron, 2006). However, the effect of antler mass on male deer crania does not lead to increases in suture complexity compared with female white-tailed deer lacking antlers (Nicolay & Vaders, 2006).

If sutures do act like fault lines for absorbing mechanical strains (Jaslow, 1990; Jaslow & Biewener, 1995), then anatomical landmarks such as bregma and lambda (where calvarial sutures such as coronal, sagittal and lambdoid sutures meet) are expected to exhibit greater complexity in animals fed a mechanically demanding diet. An additional

positive correlate for this diet type is jaw size, and has been studied in primates as mandibular corpus thickness and cross-sectional area (Daegling, 1992; Anapol & Lee, 1994; Byron, 2009). Here, we report on a mouse model system that has been used to experimentally alter feeding conditions in order to test some basic predictions concerning form and function in the vertebrate cranium. One hypothesis states that suture complexity and mandible size will positively interact with the masticatory demand of diet. A corollary and null hypothesis states that these variables are not impacted by dietary material properties. Each landmark occupies a distinct region of interest (ROI) along the skull-cap's antero-posterior axis, with bregma associated with a more anterior region and lambda associated with a posterior region. It is predicted that diets with greater mechanical demands will be associated with increased suture complexity. Furthermore, the posterior calvarial ROI, lambda is expected to associate more strongly with masticatory function. The rationale for this prediction lies in the fact that chewing muscles insert towards the posterior calvarium and not towards the anterior region (bregma).

Materials and methods

Weanling female mice from the CD-1 (ICR) strain were obtained from Charles River Laboratories (Wilmington, MA, USA). This mouse strain is representative of a standard outbred albino mouse. Subjects were randomly assigned to one of two feeding groups at 21 days postnatal ($n = 16$ per group) and raised to maturity for 10 weeks until approximately 3.5 months old (i.e. adult). Feeding groups contrast with respect to their diversity of material properties and variation in fibrous qualities. The masticatory overuse group was given access to a wire cage lid, pelleted rodent chow, shelled and unshelled pecans and walnuts, pumpkin seeds, cotton bedding squares, and access to a water bottle and sipper tube *ad libitum*. These conditions represent an enriched feeding habit allowing each test subject a lifetime of diverse materials to probe, test and comminute with their masticatory system. The masticatory underuse group was deprived of this dietary habit, and sources of chew materials (e.g. water sipper tube and wire cage top) were removed. Instead, the underuse group was fed Diet Gel[®] 76A (Clear H₂O) throughout the experiment. Mice were weighed weekly and monitored for severe weight loss (i.e. does not exceed 20% of previous recorded mass), which would have disqualified them from the study. Table 1 demonstrates that body mass at the end of the experiment was significantly larger in the overuse group by about 10% of overall mass compared with the underuse dietary group [body mass (g), $P < 0.001$]. This was expected considering that the underuse group only received hydration through the gel food, and had no access to a water source. All mice were used according to the guidelines provided by Mercer's Institutional Animal Care and Use Committee (IACUC#A1308012), and were killed by sedation followed with paraformalin perfusion.

Animals were weighed upon death to the nearest 0.1 g. Temporalis muscles were dissected and weighed to the nearest 0.001 g. The mandible was dissected free and cleaned of soft tissue. Mandibles were embedded in methyl methacrylate plastic, and histological sections were cut along the cheek tooth row of the mandibular corpus (Fig. 1). Approximately five-eight sections

Table 1 Descriptive and test statistics.

Dependent variable	Overuse (n = 18)		Underuse (n = 16)		t-stat	df	P-value
	Mean	SD	Mean	SD			
Body mass (g)	32.66	2.67	29.35	2.36	3.79	30.89	< 0.001
Corpus mean area molar section (mm ²)	3.75	0.38	3.17	0.31	4.92	31.74	< 0.001
Masseter mass (g)	0.13	0.03	0.12	0.01	0.78	11.55	NS
Normalized masseter mass (%)	0.39	0.09	0.41	0.05	-0.48	11.04	NS
Temporalis mass (g)	0.04	0.01	0.04	0.01	1.22	13.31	NS
Normalized temporalis mass (%)	0.13	0.04	0.12	0.04	0.28	13.82	NS
Lambda pathlength (mm)	10.15	1.47	8.69	1.62	2.75	30.50	< 0.05
Lambda chord length (mm)	6.13	0.32	6.06	0.18	0.76	27.53	NS
Lambda area (mm ²)	1.01	0.18	0.91	0.20	1.48	30.34	NS
Lambda width (mm)	0.10	0.01	0.11	0.02	-1.09	23.84	NS
Lambda RL (ratio)	1.66	0.27	1.43	0.27	2.50	31.56	< 0.05
Bregma pathlength (mm)	9.50	0.88	9.72	0.68	-0.85	31.43	NS
Bregma chord length (mm)	7.79	0.20	7.86	0.33	-0.75	23.90	NS
Bregma area (mm ²)	0.86	0.15	1.01	0.18	-2.58	28.97	< 0.05
Bregma width (mm)	0.09	0.02	0.10	0.02	-1.99	31.17	NS
Bregma RL (ratio)	1.22	0.11	1.24	0.10	-0.53	31.96	NS

P-values that are deemed significant are presented in bold font.

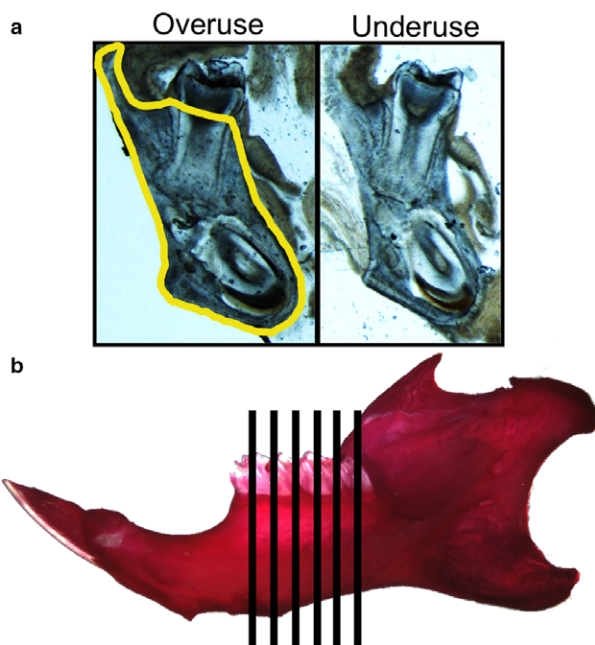


Fig. 1 Here, views of mandibular corpus cross-sections are compared from each group. Cross-sections (a) are cut from the corpus at multiple coronal planes along the mesial-distal length of the cheek teeth (black lines in b). The alizarin red stain of the whole mandible (b) is only for imaging purposes. The yellow outline on the overuse specimen slice demonstrates the method for tracing out the area measurement on each unstained section. For each individual mouse, the cross-sectional area of the multiple coronal sections was averaged. Only the tooth crown was excluded from each tracing because it extends away from the corpus and is not considered within the body of the mandible.

were taken, each with a thickness of about 250–350 μm . The five or six corpus sections that were individually observed to contain a portion of the molar teeth were selected per specimen and imaged at 10 \times magnification. This area for each histo-section was then averaged per specimen making it a secure estimate of jaw size, specifically where the molar teeth are. If increased dietary forces are shaping the skeletal connective tissues of the crania, we expect the mandible to show a larger size. Mouse calvaria were cleaned and stained with water-soluble Evan's Blue dye (Hamer et al. 2002). This is easily absorbed by the exposed collagenous extracellular matrix and marks the soft tissue zone of the cranial sutures. Under the microscope, pictures were saved as tiff image files for the bregma ROI and the lambda ROI at 20 \times magnification (Nikon SMZ800).

Using select and measurement tools within ImageJ (Fiji) 2.0, image files representing mandibular cross-sections in plastic, as well as bregma and lambda ROIs stained with Evans Blue dye, were measured for each specimen in the study. Mandibular size (mm²) was taken as the mean of areas along the molar tooth row from each individual. Coronal, sagittal and lambdoid sutures were traced and measured for each ROI in order to quantify suture pathlength, chord length and suture area (Fig. 2). The mean, standard deviation, t-statistic and significance probability of each variable were evaluated and visualized using RStudio version 1.0.136 [t.test(variable ~ treatment group), tapply(variable, treatment group, sd), ggplot(x=treatment group, y=variable) + geom_boxplot()]. A t-test comparing independent sample means was carried out for each variable. All linear measurements (traced in ImageJ) are from an ectocranial perspective in mm and area measures are in mm². Ratios are unit-free. Suture relative length (RL) is calculated by dividing absolute suture pathlength (or sinuosity) by the suture chord length. This ratiometric variable denotes suture morphology from an ectocranial perspective and is also referred to as 'sinuosity index' (Markey et al. 2006; Markey &

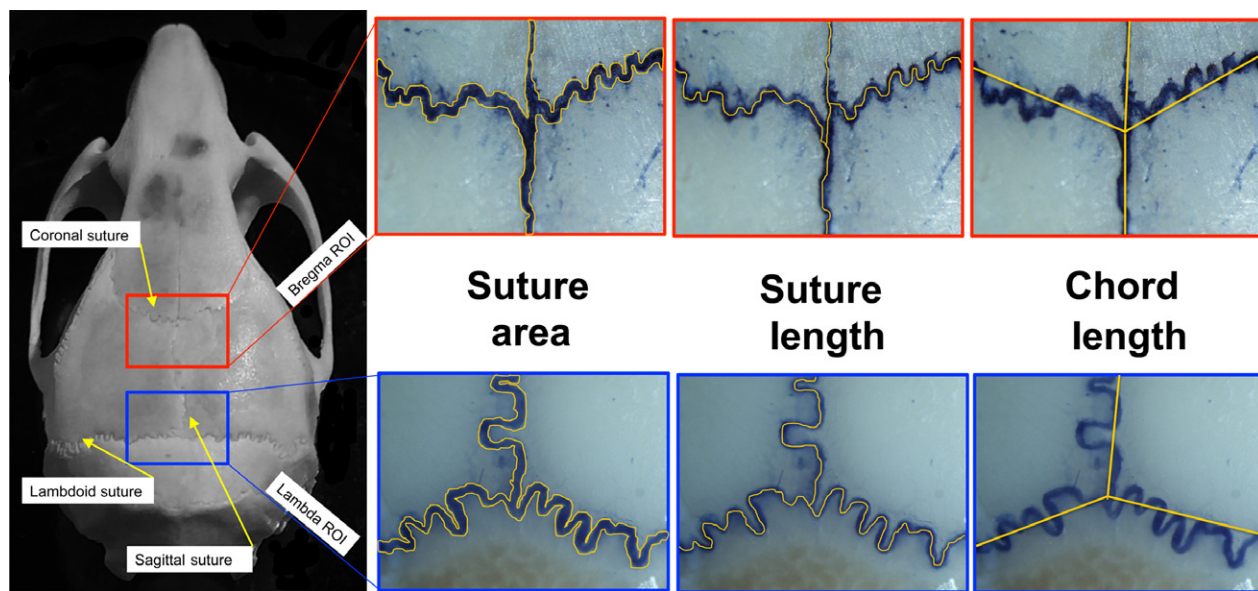


Fig. 2 A typical mouse cranium is depicted here with bregma and lambda suture regions of interest (ROIs). The inset photographs depict the method for measuring suture area, suture pathlength (sinuosity) and suture chord length. In red frames are the measurements pertinent to the bregma ROI from the anterior calvarium. In blue frames are the measurements of the lambda ROI from the posterior calvarium. In order to produce images for analysis that are consistent, the intersection of orthogonal sutures in each ROI was centered in the frame of the picture.

Marshall, 2007a,b). The suture pattern running perpendicular to its ectocranial complexity going from endo- to ecto-surfaces (i.e. interdigitation) was not measured in this study. Suture width was calculated by dividing the suture area by the absolute suture length (Bailleul et al. 2016).

Suture RL = Suture pathlength/Chord length

Suture width = Suture area/Suture pathlength

Results

Contrasting the feeding regime for the underuse and overuse groups had no impact on several of the variables, while four showed a significant increase in the overuse group and one showed a significant increase in the underuse group (Table 1). The overuse masticatory group had significantly larger body size compared with the underuse group probably because they relied entirely on the gel food source for hydration and thus could not drink water *ad libitum*. Despite body mass being 11% larger it did not have an impact on masticatory muscle size. Neither the masseter nor the temporalis muscles showed significant differences between experimental groups with either their raw expression (g), or as a ratio with body mass. The metric describing mandibular corpus cross-sectional area was significantly increased in the overuse group (Fig. 3a). Because this metric is the result of averaging five–six histosections each bearing a portion of a molar, it is a robust measurement of the size of the mandible precisely along the length where the molars reside (Fig. 1). In the overuse group, the average area of the corpus is 18% larger. Other studies have measured the mandibular corpus externally using calipers (Daegling, 1992; Anapol & Lee, 1994; Byron, 2009), but this

does not reflect the irregular geometry of a typical corpus in cross-section. This result obtained via histology represents a cross-sectional area that accounts for this.

Within the sutures of the calvarium, those in the anterior region (bregma) did not show many significant differences between dietary groups, while those from the posterior (lambda) region were clearly affected by the dietary regime in this experiment (Fig. 3b,c). This posterior difference of the calvarium was driven by 17% greater suture pathlength (mm) in the overuse group. This variable traces the ectocranial surface of the suture (i.e. sinuosity). Chord length (mm) was not significantly different between dietary groups (Fig. 2). A ratio between pathlength and chord length (i.e. index of sinuosity) was 16% larger in the dietary overuse animals for lambda RL (Fig. 3c; Table 1). Therefore, dietary overuse increased the sutural complexity of the lambdoid sutures and the posterior half of the sagittal suture in a way not affected by the coronal and anterior sagittal sutures. The ratio of suture complexity (lambda RL) for this posterior ROI demonstrates increasing sinuosity (both raw and as the index) of the suture in the overuse mice committed to a more mechanically demanding diet (lambda pathlength/lambda chord length = 1.66 ± 0.27 vs. 1.43 ± 0.27 ; $P < 0.05$).

Sutural area was also measured from an ectocranial perspective in the bregma and lambda ROIs. The lambda region sutures exhibited 10% greater area (mm^2) in the overuse group compared with the underuse group, but this difference was not statistically significant. The bregma region on the other hand exhibited 15% greater suture area (mm^2) in the underuse group compared with the overuse group, and this difference was statistically significant

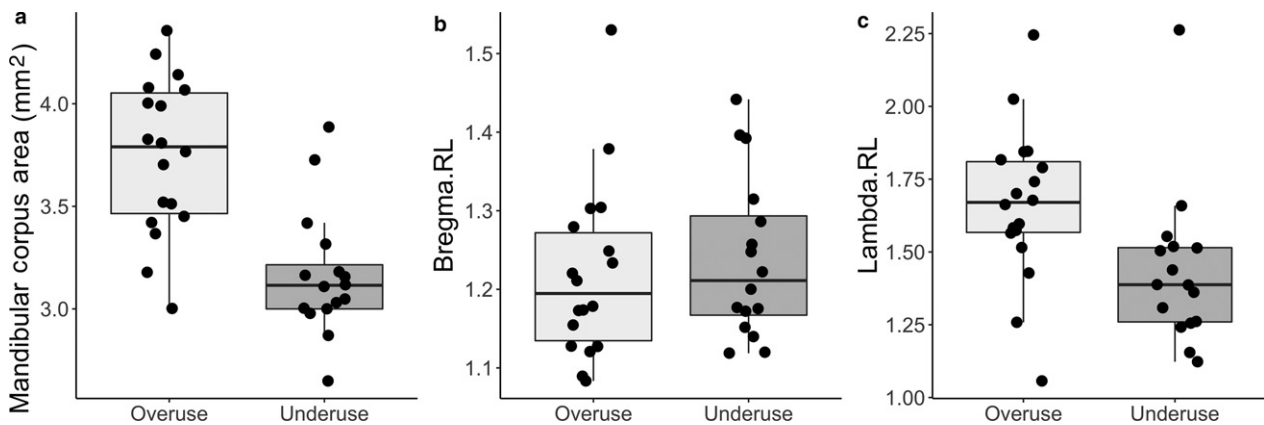


Fig. 3 Box and whisker plots compare overuse and underuse dietary groups. (a) Mandibular corpus cross-sections in mm^2 show the overuse group with significantly larger average corpus sizes ($P < 0.001$). Plots that compare suture complexity for each dietary experimental group at bregma ROI (b) and lambda ROI (c) show that suture growth at the posterior region of the mouse calvarium, and not the anterior region, is responsive to the overuse diet ($P < 0.05$).

($P < 0.05$). Quantifying the area enables one to deduce an additional linear dimension of each sutural ROI imaged and analyzed in this study. Dividing the area (mm^2) by the suture pathlength (mm) yields a dimension in the same unit as length but describing a perpendicular axis. Thus, the quotient represents the width of the suture (mm; Bailleul & Horner, 2016; Bailleul et al. 2016), and it is about 0.10 mm for each group at both the bregma and lambda regions. Suture width did not show significant differences between dietary groups. While the posterior calvarium is responsive to dietary material property demands and the anterior calvarium is not, this responsiveness is due to sutural joint growth by increasing length and not increasing width.

Discussion

Mammalian chewing is an innovative feeding behavior that often involves the handling of a food item in the mouth while it is probed, tested and reduced. Each of these behaviors acts to increase the mechanical demands placed on the cranium and associated masticatory system through greater strain magnitudes and/or greater strain frequency. Previous studies of the capuchin monkey *Cebus apella* have indicated that species adapted to eating mechanically tougher diets have more robust mandibles and greater cranial suture complexity than those committed to softer diets as measured by cranial suture pathlength (sinuosity) divided by chord length (Byron, 2009). Similarly, there is evidence that caiman alligatorids exhibit this same dietary effect on cranial sutures of the rostrum with obdurate foods being related to greater suture sinuosity and fractal complexity (Monteiro & Lessa, 2000). Additionally, American alligators also show differences in suture complexity between wild and domestic stocks, and these two groups are known to have different diets (Bailleul et al. 2016). We therefore

anticipated that habitual masticatory overuse would, on average, result in greater growth of suture sinuosity and mandibular size than in the underuse group. The hypothesis that suture complexity/sinuosity and mandible size will positively interact with the masticatory demand of diet was supported by these data. Statistical analysis shows that there were significant increases in mandibular corpus area and sagittal and lambdoid suture sinuosity (both raw and as sinuosity index) at lambda in the overuse compared with underuse groups.

The source of influence in shaping this morphological complexity appears to be sinuosity increase observed in the overuse group, here referred to as suture pathlength. The unit of expression (mm) is the numerator in the ratio lambda RL, or sinuosity index (Markey & Marshall, 2007a,b). Chord length is the denominator (mm) and has a lower standard deviation per group compared with other variables because the landmark coordinates that define the lambda, sagittal and coronal suture chord length lines are the same for all specimens regardless of group. Thus, the increased suture complexity at the lambdoid and sagittal sutures is predicted to involve more sutural cells and extracellular matrix along the ectocranial length of the joint. We speculate that this is a growth result for dense regular connective tissue throughout a lifetime of masticatory forces transmitting to these ROIs.

Naturally, increasing the pathlength of the suture in the lambda ROI adds to the measurement of ectocranial suture area (Table 1), although this 10% increase is not significant. Unexpectedly, the bregma ROI was significantly different between dietary groups, with the underuse group showing 15% greater suture area. It is not clear why this result was observed for the bregma ROI. It is worth noting that the bregma ROI pathlength also trended larger in the underuse group compared with the overuse group, but this variable was not significantly different between dietary groups. If

this significant finding in the bregma ROI of decreased area in the overuse group is not spurious then it might relate to some kind of 'rebounding' effect in an opposite region from where the primary forces of mastication are experienced (i.e. the lambda ROI). There is no way to test this assertion given the present study, but additional experiments using strain gages at multiple sagittal suture sites would be informative.

Measurement of the variable suture area enables the calculation of a standard suture width based on the entire ROI (area mm²/length mm = width mm). Suture width did not show any difference between dietary groups or between anterior and posterior calvarial ROIs. For each suture region and dietary group a standard coefficient of variation was observed (suture width standard deviation * 100/suture width mean \cong 10–20%). Thus, the typical width of the mouse calvarial suture in this study is about 100 μ m (0.1 mm). Studies of human calvarial sutures indicate a $\sim 10 \times$ larger width of ~ 0.9 – 1.3 mm (Soboleski et al. 1997; Eley et al. 2013). Rats on the other hand exhibit a somewhat similar calvarial suture width ($\sim 3 \times$) to mice at ~ 0.3 mm, and this width stays very constant throughout maturation and adulthood (Proff et al. 2006). Thus, the mouse calvarial suture width of ~ 0.1 mm has only a few fibroblast cells spanning this gap. If suture pathlength elongates in response to mechanical loading, then it can also be interpreted that width stays constant, not affected by such forces.

A limitation of this study is the lack of brain mass or volume as a proxy for cranial capacity. Because of this we are unable to speculate whether brain size interacts with the suture morphology measures observed here. Through analyzing bregma and lambda as two distinct ROIs, we incorporated information from five sutures of the calvarium that all converge at the cranial midline. Presumably mechanical loads get transmitted to these epicenters (or focal points) from the bilaterally paired muscles of mastication such as masseter and temporalis. These results support the hypothesis that in the mouse, the lambda ROI acts as a 'strain sink' during chewing behaviors, while the bregma ROI does not. The bregma ROI, however, may play a role in mechanical loads from other non-masticatory functions. Regional variation was seen across the skull in rodent taxa utilizing fossorial habits with rostral sutures significantly more complex in rodent families Ctenomyidae and Octodontidae (Buezas et al. 2017). These taxa exhibit chisel-tooth digging and burrowing behaviors that likely place increased mechanical demands on the premaxillofrontal sutures leading to greater complexity there. We predict that masticatory strains will mostly transmit to the posterior regions of the calvarium in rodent taxa as the result of masseter and temporalis muscle action during obdurate feeding, and should be expected in other hard object feeding taxa with rostrally projecting facial prognathism.

Broadly throughout nature, using a sutured interface in a biological tissue is known to be effective in mitigating and dissipating mechanical strain (Jaslow, 1990; Jaslow & Biewener, 1995; Curtis et al. 2013; Maloul et al. 2014; Zhang & Yang, 2015; Lee et al. 2017; Liu et al. 2017). Functionally, suture complexity attenuates longitudinally directed strain wave energy traveling through rigid bones by dispersing and transforming longitudinal wave energy into transverse and shear directions. In addition, the viscoelastic nature of the suture connective tissue also dampens traveling stress waves (Lee et al. 2017). This complexity can be found beyond cranial sutures in other vertebrates, such as in a woodpecker's beak (Lee et al. 2014) or a turtle's carapace (Krauss et al. 2009). Even invertebrates have evolved structural complexity (e.g. fossil ammonite shells) for likely similar biomechanical reasons (Allen, 2007). Our study here is congruent with most other work on suture biology. We speculate that increased complexity of the sutures leading to the lambda anatomical landmark (sagittal as well as right and left lambdoid sutures) may simply be a function of masticatory overuse within the constraints of a typical rodent skull. As such the strain sink epicenters for masticatory use may be found in different regions across other vertebrate clades that possess contrasting cranial morphology.

Acknowledgements

The authors thank Mercer University's office of the Provost and the Department of Biology for the funding necessary for this project.

Conflict of interests

No conflict of interests exists in the publication of this manuscript.

Author contributions

The authors of this manuscript made differing contributions towards its completion. CB conceived of the study, analyzed/interpreted the data, and wrote/edited the manuscript. MS acquired the data, analyzed/interpreted the data, and wrote/edited the manuscript. K Herman, K Hawkinson and SP all acquired the data and analyzed/interpreted the data.

References

- Allen EG (2007) Understanding ammonoid sutures: new insight into the dynamic evolution of paleozoic suture morphology. In: *Cephalopods Present and Past: New Insights and Fresh Perspectives*. (eds. Landman NH, Davis RA, Mapes RH), pp. 159–180. Netherlands, Dordrecht: Springer.
- Anapol F, Lee S (1994) Morphological adaptation to diet in platyrrhine primates. *Am J Phys Anthropol* **94**, 239–261.
- Bailleul AM, Horner JR (2016) Comparative histology of some craniofacial sutures and skull-base synchondroses in non-avian

- dinosaurs and their extant phylogenetic bracket. *J Anat* **229**, 252–285.
- Bailleul AM, Scannella JB, Horner JR, et al. (2016) Fusion patterns in the skulls of modern Archosaurs reveal that sutures are ambiguous maturity indicators for the Dinosauria. *PLoS ONE* **11**, e0147687.
- Buezas G, Becerra F, Vassallo A (2017) Cranial suture complexity in caviomorph rodents (Rodentia; Ctenohystrica). *J Morphol* **278**, 1125–1136.
- Byron CD (2006) Role of the osteoclast in cranial suture wave-form patterning. *Anat Rec A Discov Mol Cell Evol Biol* **288**, 552–563.
- Byron CD (2009) Cranial suture morphology and its relationship to diet in *Cebus*. *J Hum Evol* **57**, 649–655.
- Byron CD, Borke J, Yu J, et al. (2004) Effects of increased muscle mass on mouse sagittal suture morphology and mechanics. *Anat Rec A Discov Mol Cell Evol Biol* **279A**, 676–684.
- Cuff AR, Bright JA, Rayfield EJ (2015) Validation experiments on finite element models of an ostrich (*Struthio camelus*) cranium. *PeerJ* **3**, e1294.
- Curtis N, Jones MEH, Evans SE, et al. (2013) Cranial sutures work collectively to distribute strain throughout the reptile skull. *J R Soc Interface* **10**, 20130442.
- Daegling DJ (1992) Mandibular morphology and diet in the genus *Cebus*. *Int J Primatol* **13**, 545–570.
- Eley KA, Sheerin F, Taylor N, et al. (2013) Identification of normal cranial sutures in infants on routine magnetic resonance imaging. *J Craniofac Surg* **24**, 317–320.
- Farke AA (2008) Frontal sinuses and head-butting in goats: a finite element analysis. *J Exp Biol* **211**, 3085–3094.
- Hamer PW, McGeachie JM, Davies MJ, et al. (2002) Evans Blue Dye as an in vivo marker of myofibre damage: optimising parameters for detecting initial myofibre membrane permeability. *J Anat* **200**, 69–79.
- Herring SW (1972) Sutures—a tool in functional cranial analysis. *Acta Anat (Basel)* **83**, 222–247.
- Herring SW, Mucci RJ (1991) In vivo strain in cranial sutures: the zygomatic arch. *J Morphol* **207**, 225–239.
- Hylander WL, Johnson KR, Crompton AW (1987) Loading patterns and jaw movements during mastication in *Macaca fascicularis*: a bone-strain, electromyographic, and cineradiographic analysis. *Am J Phys Anthropol* **72**, 287–314.
- Jasinowski SC, Rayfield EJ, Chinsamy A (2010) Functional implications of dicynodont cranial suture morphology. *J Morphol* **271**, 705–728.
- Jaslow CR (1990) Mechanical properties of cranial sutures. *J Biomech* **23**, 313–321.
- Jaslow CR, Biewener AA (1995) Strain patterns in the horncores, cranial bones and sutures of goats (*Capra hircus*) during impact loading. *J Zool* **235**, 193–210.
- Khonsari RH, Olivier J, Vigneaux P (2013) A mathematical model for mechanotransduction at the early steps of suture formation. *Proc Biol Sci R Soc* **280**, 20122670.
- Krauss S, Monsonego-Ornan E, Zelzer E (2009) Mechanical function of a complex three-dimensional suture joining the bony elements in the shell of the red-eared slider turtle. *Adv Mater* **21**, 407–412.
- Lee N, Horstemeyer MF, Rhee H, et al. (2014) Hierarchical multi-scale structure-property relationships of the red-bellied woodpecker (*Melanerpes carolinus*) beak. *J R Soc Interface* **11**, 20140274.
- Lee N, Williams L, Mun S (2017) Stress wave mitigation at suture interfaces. *Biomed Phys Eng Express* **3**, 35025.
- Liu L, Jiang Y, Boyce M, et al. (2017) The effects of morphological irregularity on the mechanical behavior of interdigitated biological sutures under tension. *J Biomech* **58**, 71–78.
- Maloul A, Fialkov J, Wagner D, et al. (2014) Characterization of craniofacial sutures using the finite element method. *J Biomech* **47**, 245–252.
- Mao JJ (2002) Mechanobiology of craniofacial sutures. *J Dent Res* **81**, 810–816.
- Markey MJ, Marshall CR (2007a) Terrestrial-style feeding in a very early aquatic tetrapod is supported by evidence from experimental analysis of suture morphology. *Proc Natl Acad Sci USA* **104**, 7134–7138.
- Markey MJ, Marshall CR (2007b) Linking form and function of the fibrous joints in the skull: a new quantification scheme for cranial sutures using the extant fish *Polypterus endlicherii*. *J Morphol* **268**, 89–102.
- Markey MJ, Main RP, Marshall CR (2006) In vivo cranial suture function and suture morphology in the extant fish *Polypterus*: implications for inferring skull function in living and fossil fish. *J Exp Biol* **209**, 2085–2102.
- Monteiro LR, Lessa LG (2000) Comparative analysis of cranial suture complexity in the genus *Caiman* (Crocodylia, Alligatoridae). *Braz J Biol* **60**, 689–694.
- Moss ML (1997a) The functional matrix hypothesis revisited. 1. The role of mechanotransduction. *Am J Orthod Dentofac Orthop* **112**, 8–11.
- Moss ML (1997b) The functional matrix hypothesis revisited. 2. The role of an Osseous connected cellular network. *Am J Orthod Dentofac Orthop* **112**, 221–226.
- Moss ML (1997c) The functional matrix hypothesis revisited. 3. The genomic thesis. *Am J Orthod Dentofac Orthop* **112**, 338–342.
- Moss ML (1997d) The functional matrix hypothesis revisited. 4. The epigenetic antithesis and the resolving synthesis. *Am J Orthod Dentofac Orthop* **112**, 410–417.
- Nicolay CW, Vaders MJ (2006) Cranial suture complexity in white-tailed deer (*Odocoileus virginianus*). *J Morphol* **267**, 841–849.
- Proff P, Weingärtner J, Bayerlein T, et al. (2006) Histological and histomorphometric study of growth-related changes of cranial sutures in the animal model. *J Craniomaxillofac Surg* **34**, 96–100.
- Rafferty KL, Herring SW (1999) Craniofacial sutures: morphology, growth, and in vivo masticatory strains. *J Morphol* **242**, 167–179.
- Soboleski D, McCloskey D, Mussari B, et al. (1997) Sonography of normal cranial sutures. *Am J Roentgenol* **168**, 819–821.
- Sun Z, Lee E, Herring SW (2004) Cranial sutures and bones: growth and fusion in relation to masticatory strain. *Anat Rec A Discov Mol Cell Evol Biol* **276A**, 150–161.
- Weijjs WA, de Jongh HJ (1977) Strain in mandibular alveolar bone during mastication in the rabbit. *Arch Oral Biol* **22**, 667–675.
- Zhang ZQ, Yang JL (2015) Biomechanical dynamics of cranial sutures during simulated impulsive loading. *Appl Bionics Biomech* **2015**, 1–11.
- Zollikofer CPE, Weissmann JD (2011) A bidirectional interface growth model for cranial interosseous suture morphogenesis. *J Anat* **219**, 100–114.